F.O. Clark, R. Penny, J.A. Cline, W.E. Pereira, and J. Kielkopf, A Passive Optical Technique to Measure Physical Properties of a Vibrating Surface, Proc. SPIE 9219, Infrared Remote Sensing and Instrumentation XXII, 92190G, 2014.

doi: 10.1117/12.2064366

See next page.

A Passive Optical Technique to Measure Physical Properties of a Vibrating Surface

Frank O. Clark, Ryan Penney, Spectral Sciences, Inc., 4 Fourth Ave., Burlington, MA, 01803, Wellesley E. Pereira, Air Force Research Laboratory RVB, Kirtland AFB, NM 87117, John Kielkopf, Department of Physics and Astronomy, University of Louisville, Louisville, KY 40292, Jason Cline, Spectral Sciences, Inc., 4 Fourth Ave., Burlington, MA, 01803.

ABSTRACT

We report on a passive imaging technique to measure physical properties of a vibrating surface using the detection of optical signal modulation in light scattered from that surface. The optical signal modulation arises from a changing surface normal and may be used to produce a surface normal change image without touching the surface and changing its state. The images may be used to extract the surface vibration frequency and mode pattern which are dependent on surface properties of the material, including its flexural modulus and mass density. Comparison of the vibration image with a finite element model may be used to infer properties of the vibrating surface, including boundary conditions. A temporal sequence of optical images of signal modulation may be analyzed to infer spatial damping properties of the surface material. Damping is a measure of energy dissipation within the material. The approach being developed has the advantage of being able to remotely image arbitrary sized structures to determine global or local vibrational properties.

Keywords: passive, optical, surface vibration, surface normal deflection

Paper 9219-16

Address correspondence to Frank O. Clark, fclark@spectral.com

1. LIGHT SCATTERING – GENERAL AND TEMPORAL MODULATION

The foundations for this work are found in a series of public patents by Clark (section 3) and very early results are described in the document by Pereira et al. (section 3).

Nicodemus et al. [1] provide a complete geometrical optics treatise on reflectance, and defined relevant essentials of reflectance, first introducing the term bidirectional reflectance distribution function (BRDF). "The BRDF is a derivative, a distribution function, relating the irradiance incident from one given direction to its contribution to the reflected radiance in another direction." Nicodemus *et al*'s BRDF does not contain artificial "specular and diffuse" components, *per se*, it describes the reflected light without subdivision. A BRDF is a multidimensional surface. The relevant variables are not only the angle and solid angle of both illumination and observation, but also wavelength, polarization, and, of interest here, temporal modulation. Again to quote Nicodemus: "***Reflection*** is the process by which electromagnetic flux (power), incident on a stationary surface or medium, leaves that surface or medium from the incident side without change in frequency; ***reflectance*** is the fraction of the incident flux that is reflected." Nicodemus defines more complex scattering descriptors, but we will use BRDF as sufficient for this task, and BRDF is $f(\theta_i, \phi_i, \theta_r, \phi_r)$ (defined in Figure1), where i is incident and r is reflected (Figure 1). It is understood that actual measurements are not made at infinitesimal solid angle. The incident and reflected flux are integrated over the solid angle of the illuminating source as seen by the reflecting surface and integrated over the solid angle subtended by the detector.

A surface vibration change will change the surface normal of each infinitesimal unit surface area (dA in figure 1) and therefore projected area and irradiance (power per unit area). Thus a vibration in a surface will cause corresponding changes in the irradiance of each infinitesimal unit area (dA) across the surface. This change in irradiance, as we will show, will produce a modulation in light that is diffusely scattered across that surface, even for a perfectly Lambertian scattering surface.

Infrared Remote Sensing and Instrumentation XXII, edited by Marija Strojnik Scholl, Gonzalo Páez, Proc. of SPIE Vol. 9219, 92190G · © 2014 SPIE
CCC code: 0277-786X/14/$18 · doi: 10.1117/12.2064366

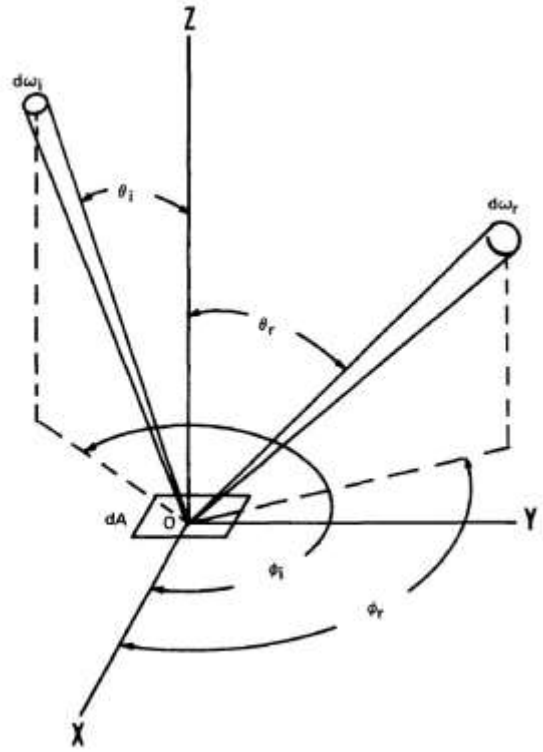

Figure 1. Nicomdemus' general geometry (NIST, public domain)

2. LIGHT SCATTERING OVERVIEW

We discuss a few aspects key to the theory on optical modulation of light, focusing on low contrast vibrating surfaces. We emphasize at the outset that specular reflection is a special case, and our primary interest is in non-specular reflection, that is to say scattering into any arbitrary direction. The scattering surface itself may exhibit structure as shown in Figure 2, and all or part may be vibrating.

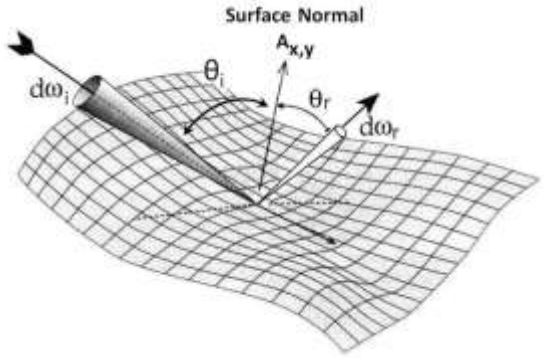

Figure 2. General complex curved surface

The complexity of the BRDF of common materials is well known. For example, as shown by a 3-dimensional surface plot in Fig. 3, Mauer [2] reveals that light scattering from blades of grass can be spatially anisotropic. Implicitly, the BRDF contains even more variables than those shown in Figure 3. For example, the BRDF will change with wavelength in a way that depends on the composition the material as illustrated in Fig. 4.

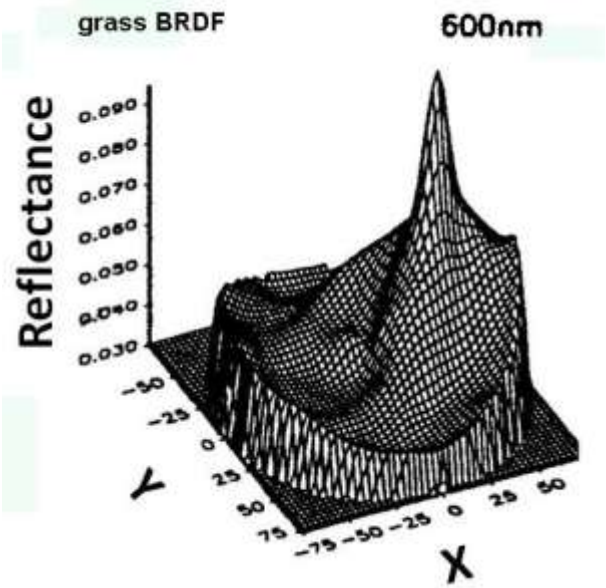

Figure 3. BRDF of grass from Mauer[3], used with permission

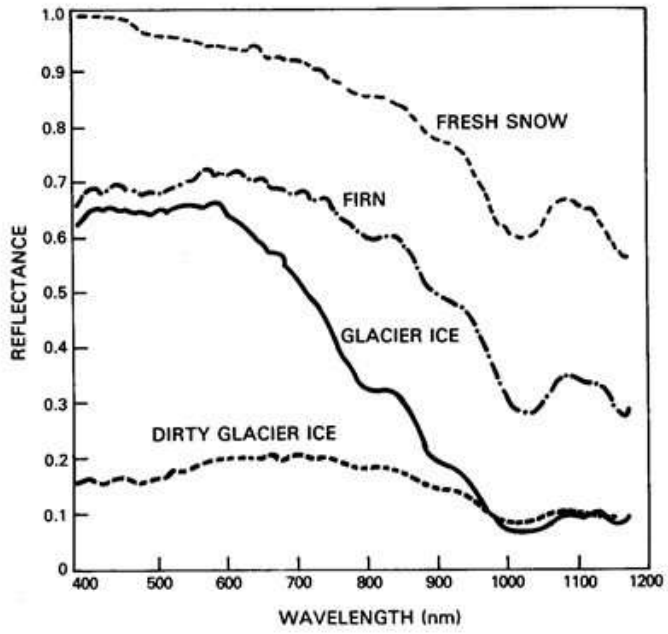

Figure 4. Spectral reflectivity various surfaces (Mauer[3], used with permission)

Further, as we will touch on in section 5, the BRDF is a function representing the aggregate behavior of scattering from unresolved structure. Thus the BRDF will depend on the spatial resolution of the measuring instrument compared to a scale length for apparent homogeneity of the observed material.

In summary, although "BRDF" is often illustrated as an ideal two dimensional plot, it is in practice a very complex multi-dimensional feature of scattering from surfaces potentially exhibiting isotropic or anisotropic polarization properties and wavelength variability. As in the case of interest here, if the scattering surface has temporal

variability, the temporal characteristics of all of these components of the BRDF are of interest in optimizing the detected variation.

3. DETECTING TEMPORAL CHANGES in OPTICAL SIGNAL MODULATION

A method of detecting modulation in light diffusely scattered from vibrating surfaces was discovered by Clark [3,4,5]. The detected intensity modulation levels may be very small, often one part in 10^5. First results are described in Pereira *et al.*[6]. Detection of modulation in diffuse scattered light may be done with any orientation of the source or observer. It is known from laboratory and field measurements that a ubiquitous effect from low contrast (nearly uniform BRDF) vibrating surfaces, which we might term *bulk surface modulation* is associated with small localized changes in surface normal (angle). These laboratory experiments show this passive approach to be about five times more sensitive than laser vibrometry at low frequencies, and to operate at much greater distances (it is single pass through the atmosphere), although it is to be emphasized that the two techniques do not measure the same phenomena (as will be discussed below). Non-Lambertian structured BRDFs, i.e., specular surfaces, provide further enhancements of the signal, especially near the glint lobe. Fractional modulation signals as low as 10^{-5} (nearly Lambertian) and as high as nearly 0.2 (20%)(non-Lambertian) of the ambient radiance have been detected using focal plane arrays of high dynamic range with large well depths and moderate resolution analog-to-digital converters. Some of these are described in an application for detecting vibrations through contrast features (edge detection) Hay et al. [7] Kielkopf and Hay [8]. While it is not necessary to understand the details of a non-Lambertian BRDF to detect surface vibration phenomena, an accurate model incorporating physics-based non-Lambertian BRDF temporal effects offers an advantage by potentially showing how to utilize this multidimensional variability space to increase the detectable intensity modulation, thus increasing sensitivity of the technique.

4. THEORY OF OPTICAL DETECTION OF SURFACE VIBRATION

Let us start by modeling the simplest surface. The vibration of a low contrast unpatterned Lambertian scattering surface will modulate the intensity of scattered light primarily through changes in the surface normal vector (Figures 1, 2, and 5). Even with a theoretically pure Lambertian scattering surface, light intensity will scale with the cosine of the angle of illumination Θ_i (Figure 1 and 2), the angle between the illumination source and the surface normal, because of the change in projected differential surface area, *dA* (Figure 1), i.e. the irradiance on that projected differential surface area will change (Figure 1 and 2). More common structured (non-Lambertian) BRDFs (Figure 3) may increase intensity changes from surface vibration. We may quantitatively model the time dependence of light intensity scattered from a surface and detected by an observer as a time derivative with respect to key variables given by

$$\left(\frac{\partial I}{\partial t}\right) = \left(\frac{\partial I}{\partial \Omega_i}\right)\left(\frac{\partial \Omega_i}{\partial t}\right) + \left(\frac{\partial I}{\partial \Omega_r}\right)\left(\frac{\partial \Omega_r}{\partial t}\right) \tag{1}$$

Where:

I is intensity through a differential surface area of the detector.

Ω_i is the solid angle of the illumination source (Figure 1 and 2)

Ω_r is the solid angle of the detector pixel (Figure 1 and 2)

We assume the illumination source, scattering object, and detector are at rest, except for scattering object surface vibrations. Motion of the illumination source, the detector, or the scattering object will introduce additional similar terms in equation 1.

The intensity scattered from a differential surface element, *dA*, located on a vibrating surface, oscillates with time. Light travels from the illumination source with solid angle Ω_i, scatters off of area element *dA* and travels into the solid angle of the detector element, Ω_r. The time dependent signal $\partial I/\partial t$ is for a given material and wavelength and is a function of the solid angle of the illumination source Ω_i on the elemental surface area *dA* and the solid angle of the detector pixel, Ω_r.

For lambertian scattering (uniform scattering in all directions) and a stationary illumination source and detector, the scattered intensity in the detector direction $\hat{\Omega}_r$ is

$$I\left(\hat{\Omega}_r, \Theta_i\right) = \rho\, F^s \cos(\Theta_i) = I(\Theta_i) \tag{2}$$

Where light is scattered into a cone of solid angle around the direction $\hat{\Omega}$, ρ is the reflectance, F^s is the illumination irradiance (power per unit area), which will change as the surface normal changes by projecting a slightly different area to the illumination source. Note from Figure 7 that temporal changes in Ω_i and Ω_r from a small surface vibration are not necessarily the same! Θ_i is the incident illumination angle (Figures 1 and 2). I is constant over variable solid angle and thus has no dependence on solid angle (Chandrasekhar [9]). The derivative with respect to time is

$$\left(\frac{\partial I}{\partial t}\right) = \left(\frac{\partial I}{\partial \Theta_i}\right)\left(\frac{\partial \Theta_i}{\partial t}\right) \tag{3}$$

and the time integration for I is:

$$I(t_f) - I(t_i) = \int_{t_i}^{t_f} \left(\frac{\partial I}{\partial \Theta_i}\right)\left(\frac{\partial \Theta_i}{\partial t}\right) dt \tag{4}$$

If we assume a harmonic oscillator surface vibration with an exponential decay, not unreasonable for a point excitation with damping, then Θ as a function of spatial offset from the oscillation centroid, r, is given by:

$$\Theta(r,t) = \Theta_o + Ae^{-ar}\sin(\omega r - ft\pi) \tag{5}$$

$where\ r = \sqrt{(x-x_o)^2 + (y-y_o)^2}$, A is the maximum displacement of Θ, a is chosen to match the spatial extent of the data, ω=2π/λ is the frequency of the surface wave, λ is the wavelength of the surface wave, and *ft* is the time dependent phase. The displacement of theta (Θ) is related to the displacement of the surface normal of the unit area, $d\mathbf{A}_{x,y}$ (Figure 1), through the angular frequency by $\mathbf{A} = \omega\ \mathbf{A}_{x,y}$. The dynamic range to achieve unit signal to noise ratio, assuming the detector noise is shot noise limited, is the non-varying component of equation (5) divided by the time derivative of equation (5) (equation 4) which yields:

$$\frac{non-varying}{RMS\ time\ varying} = \sqrt{2}\left[\frac{I(\Theta_o + Ae^{-ar}sin(\omega r))}{\rho F^s |sin(\Theta)| Ae^{-ar}} - \frac{sin(\Theta)sin(\omega r)}{|sin(\Theta)|}\right] \tag{6}$$

The time varying signal in the second term is proportional to the amplitude of the angular modulation, the angle of the illumination source (Θ_i on Figures 1 and 2) and the attenuation of the surface wave (damping). We may estimate a limiting case for this Lambertian scattering example by estimating a peak excursion value at r=0 (i.e. ignore the exponential damping term in Equation 6). The peak signal of the maximum displacement at r=0 then simplifies to:

$$\frac{RMS\ time\ varying}{non-varying} \cong \frac{A|\tan(\Theta)|}{\sqrt{2}} \tag{7}$$

Therefore the time varying signal from vibration of a Lambertian scattering surface is proportional to the surface normal displacement in radians for a given angle Θ. (Kielkopf and Clark [10]). Note that $\tan(\Theta)$ approaches infinity as Θ approaches π/2 radians. Even with these simple assumptions, one may observe considerable modulation under certain conditions.

5. NON-LAMBERTIAN TEMPORAL SURFACE CHANGES

Temporal surface changes will change the local surface normal, and therefore change the projected area towards the source and the irradiance of that surface element. This change in irradiance will produce a modulation in light that is diffusely scattered across that surface, even for a perfectly Lambertian scattering surface. For a non-Lambertian BRDF, the surface normal deflections may also sample a different part of the complex BRDF surface, and potentially increase signal modulation. Let us consider a propagating linear impulse with non-Lambertian scattering.

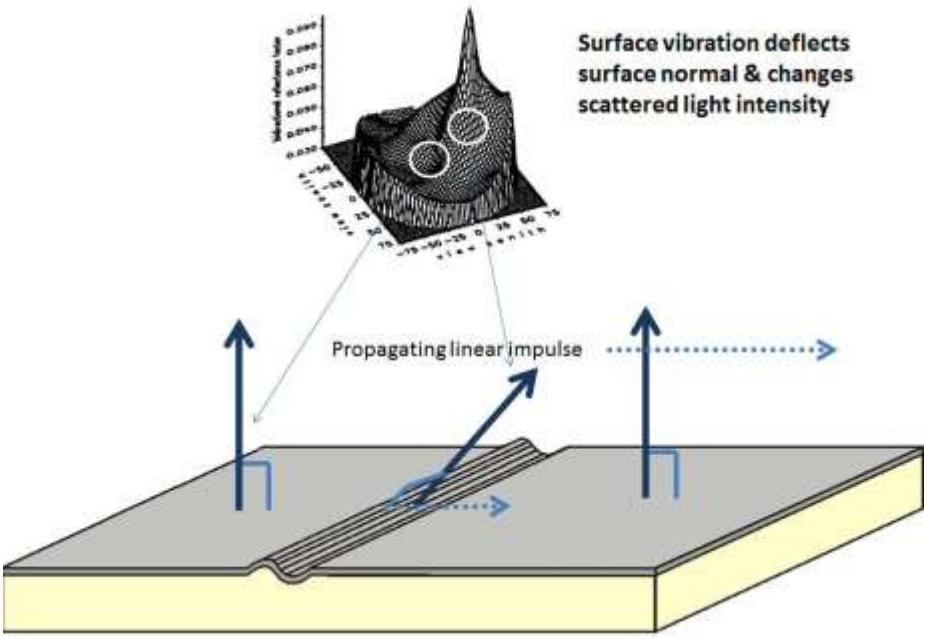

Figure 5. A propagating linear impulse with surface normal

Figure 5 illustrates that a propagating linear impulse not only changes the local surface normal and corresponding unit projected surface area and irradiance, but also has the potential to scatter light from a different area of the BRDF surface. This effect is in addition to the change in irradiance of the local unit surface area. Therefore, non-Lambertian scattering surfaces may exhibit greater scattered light modulation than the Lambertian example.

We (Kielkopf) have used these results to image a propagating impulse using optical signal modulation, as shown in Figure 6.

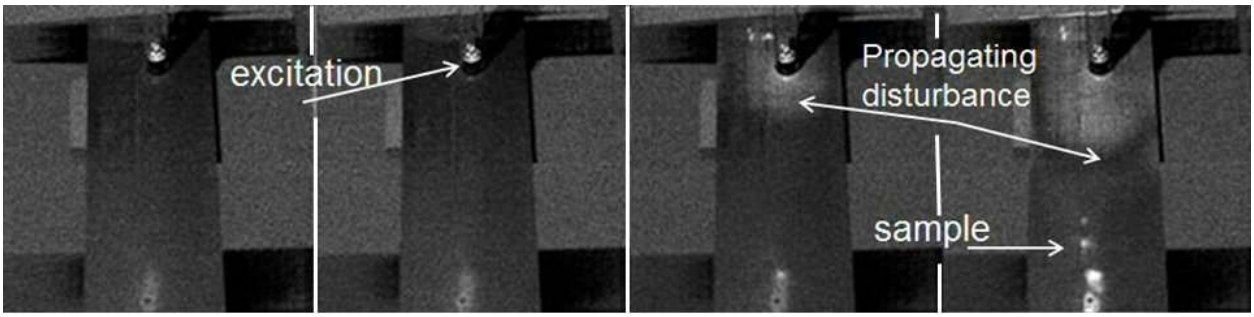

Figure 6. Imaging a propagating impulse. Four frames left to right. Image changes resulting from the impact of a falling weight on a piece of 7.62x30.48x0.159 cm composite material. The sequence from left to right are frames with cadence of 1/3000 second taken with the Photron camera at 3000 FPS. Initial contact is in frame 2.

Figure 6 shows a few frames following first contact with the falling 50 gram brass weight (frame 2) onto a 7.62x30.48x0.159 cm piece of carbon-epoxy composite (McMaster-Carr, 8194K54). The weight was held above the surface and then released from a height of approximately 1.2 meters to deliver an energy impulse of approximately 0.6 joule to the surface. Moving at approximately 5 meters per second on impact, and dissipating its energy in 1/3000 of a second, the resulting force on the surface for this brief time is 750 Newtons. The weight had a rounded nose with a flat area of approximately 0.3 cm^2 making first contact. The resulting pressure was 25 megapascals, but the brief time produced only a small surface wave that propagated away from the point of impact. Sequence left to right are derivatives with cadence of 1/3000 second (Photron camera 3000 frames per second).

Although we do not have a measured BRDF for this surface, visual inspection shows that it is not Lambertian.

The four frames shown in Figure 6 reveal the surface wave moving away from the event covering approximately 10 centimeters in a millisecond, this corresponds to a propagation velocity of roughly 100 meters per second. ***The test***

clearly demonstrates that it is feasible to image and follow the propagation of a surface disturbance using passive optical imagery. These data show that one may spatially resolve and follow the propagation of a surface disturbance using small fractional optical signal modulation from the change in surface normal.

6. BRDF TEMPORAL VARIABILITY

We have described the variation in surface normal as contributing to intensity changes in scattered light through two mechanisms, changing irradiance, and change in sampling the BRDF surface for each unit surface area. There are other physical factors contained within the term labeled as "BRDF" that contribute to changes in reflected (or scattered) intensity. Some of these are surface roughness, surface self shadowing, self masking, diffraction, interference, polarization, finite electrical conductivity, and magnetic permeability (Schlick [11]). If present, these factors may affect detectable intensity modulation, and may dominate the modulation from simple surface normal deflection. Some of these are illustrated in Figure 7.

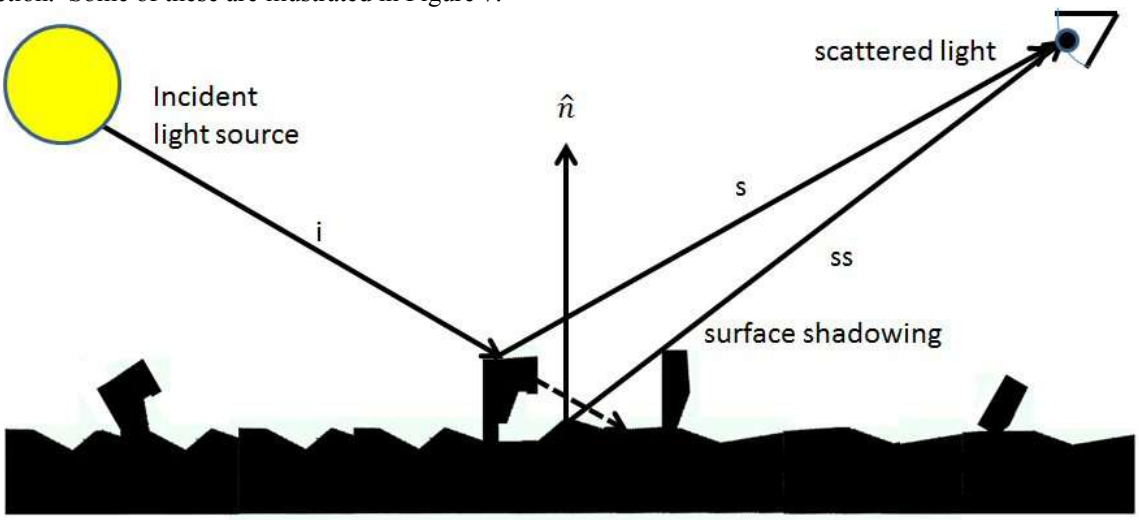

Figure 7. Geometry of reflection. $\hat{n}$ is the geometric surface normal, the incident illumination light source is shown, as is the light scattered to the observer or detection device. There are two types of "shadowing" relevant to a time varying signal in scattered light that are obvious in this figure. One prevents the line of sight from reaching the mean "surface" , marked s, and one falls on a surface area that in which the incident light source is shadowed by surface inhomogeneity, labelled ss.

To summarize the discussion of BRDF, while a physics-based BRDF model is not necessary to use scattered light as a surface vibration diagnostic, it may potentially be used to greatly increase the detectable fractional modulation. The detailed physics necessary in this non-Lambertian BRDF may be quite complex in many materials, not simply a superposition of Lambertian and specular components. We have outlined some details that may increase the detectable modulation and shown the utility of constructing complex physics based non-Lambertian BRDFs of materials.

7. STANDING WAVE PATTERNS

Let us test some of these concepts by considering optical signal modulation from a temporally varying circular membrane surface forced into 0,1 mode. As illustrated in Figure 8, surface motion deflects the surface normal at the edges, and as above, changes the irradiance and samples different areas on the BRDF surface, therefore modulating the scattered light.

The change in surface orientation may not be repetitive, may be due to an impulse, or a portion of the surface may exhibit some more regular vibration. BRDF simply scales reflected intensity at each location; and thus, the change in intensity is equal to the change in reflectance. A simplified surface vibration model describes surface orientation changes by a surface wave. For the sake of brevity, let us consider the fundamental 0,1 mode of a circular membrane.

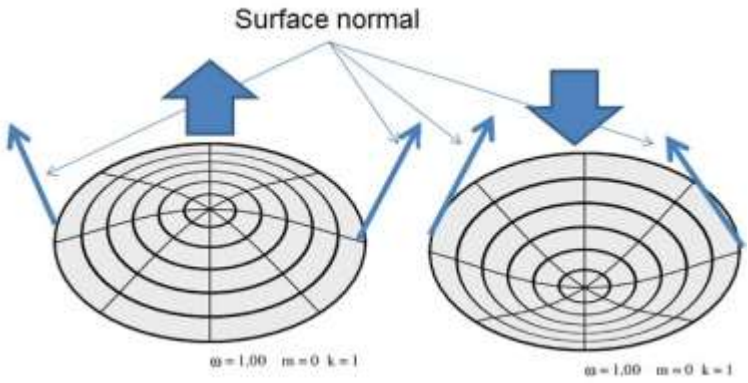

Figure 8. Circular membrane 0,1 mode, changes in surface normal maximum on periphery.

In this case, the greatest surface linear motion is in the center of the membrane, but the greatest change in surface normal occurs at the outer rim of the membrane. Thus, we expect the largest optical signal modulation to peak at the periphery, as shown in Figure 9, and should therefore exhibit as a circle or annulus peaking near the outer edge (green dashed line). Also note that while the surface normal at the center does not change, the membrane is stretched, producing a small irradiance change, and we do not expect the center to be zero modulation. We did not account for this geometrical change in our simple model. This would not affect our predicted peak modulation near the edges.

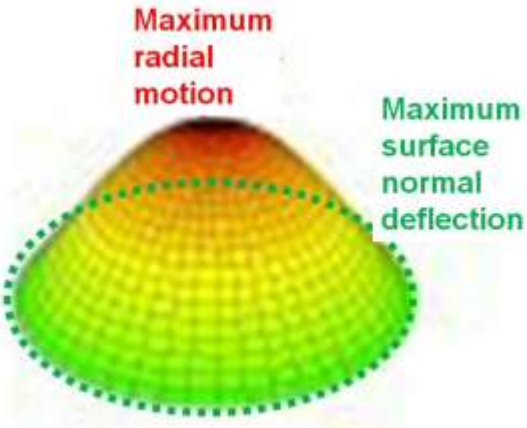

Figure 9. Circular membrane 0,1 mode vibration

In a musical drum, the 0,1 mode couples strongly to the air and dampens rapidly. Therefore in a musical drum, the 0,1 mode quickly damps out and changes modes to higher harmonic that do not couple as strongly to the air. Therefore we did a simple static experiment to illustrate this concept using a pneumatically actuated membrane stretched over a barrel. That is to say, we have forced a static 0,1 mode and not permitted mode change.

Equipment

This experiment involved imaging a latex membrane stretched over the opening of a standard 5 gallon bucket, which was then secured with a large hose clamp. The bucket has been modified with a barbed hose fitting, such that the internal volume may be connected to a small compressor or vacuum pump. This device may be seen in Figure 10. Due to the large area and low thickness of the membrane, a small pressure differential across the bucket results in a substantial deflection of the surface of the membrane.

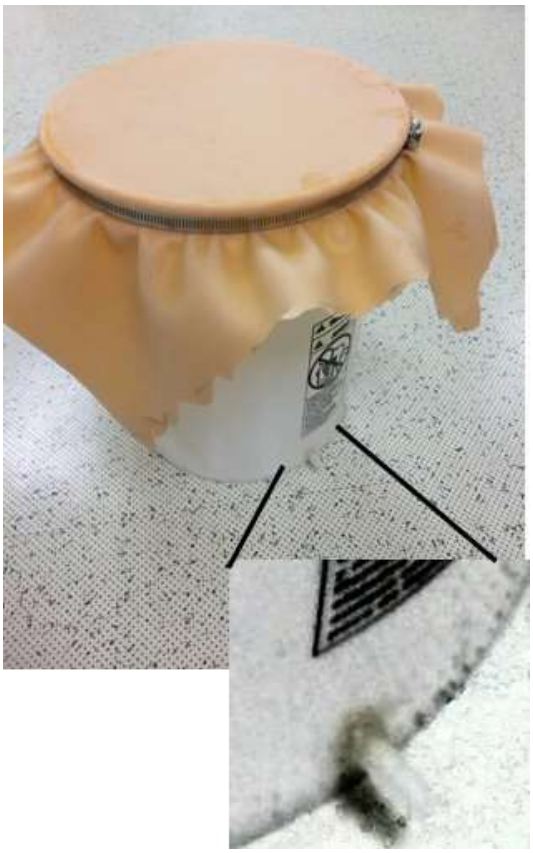

Figure 10. Latex membrane on the 5 gallon bucket. Note the hose fitting at the bottom of the bucket, shown as an inset.

The source and detector may be seen in Fig. 11. Illumination was provided with a 1000 Watt light bulb focused with an 8 inch Fresnel lens. According to the manufacturer's data sheet, the beam angle is 6.7^{o} and the efficiency is 10.3%. Imaging was performed with a Phantom v7.1 camera, equipped with a 50 mm, f/1.4 lens. Frames were collected at 100 frames per second for 250 frames, with a 10 μs exposure time. The 1000 watt illumination source is powered by 60 Hz AC; the resulting 120 Hz ripple in lamp output was negated by averaging the resulting image stacks.

Figure 11. Phantom v7.1, 10 bit, well depth 80,000 electrons, and light as placed for this experiment.

Geometry

Equipment was placed such that the source and sampling angles were as close to normal to the drum as possible. The distance from the drum head to the front lens of the camera and front lens of the source was 2.87 meters. The

camera and source were placed 15.2 cm on either side of the projected center of the drum. As a result, the camera and source were rotated approximately 3° to center on the drum, as illustrated in Figures 12 and 13.

Figure 12. Image from the rear of the experiment.

Figure 13. Image from the side of the experiment.

Data and Analysis

Data were taken with the drum at positive, zero, and negative gauge pressures. The resulting image stacks were then averaged to provide a low noise measurement. We then define fractional modulation according to Equation 8, such that the fractional modulation for these images is positive.

$$Fractional\ Modulation = \left|\frac{Flat - Deflected}{Flat}\right| \tag{8}$$

Applying this to the average images yields results shown in Figure 14 center and right for the positive and negative deflections, respectively.

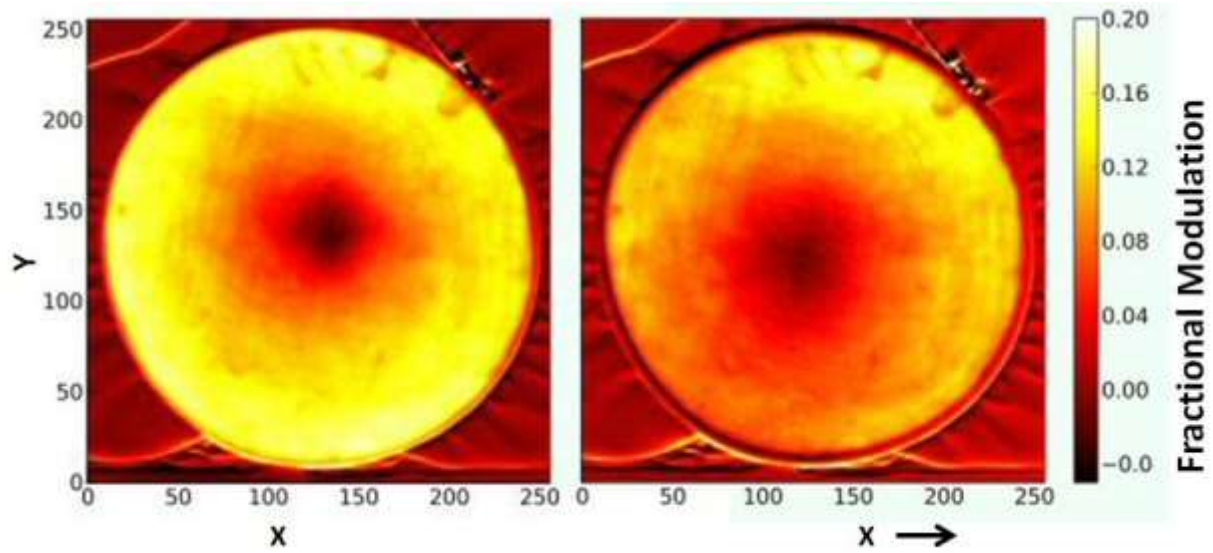

Figure 14. Fractional modulation (as defined in equation 8) of a pneumatic membrane forced into the 0,1 mode by inflating (left) and deflating (right) the membrane, relative to neutral pressure. The 3 degree offset between source and detector is responsible for the asymmetry of the modulation pattern.

Comparison of Lab Experiment to Theory

If we use our equation 7, the fractional time varying signal for an area spatially resolved by the detector pixel is approximately equivalent to $\boldsymbol{A}$, the angular displacement amplitude in radians, times the magnitude of the tangent(Θ). The experiment was done on a drum of diameter is 29.845 cm, and the membrane excursion was approximately 2.54 cm +/- 0.64 cm. The deflection in radians, $\boldsymbol{A}$, is approximately 0.34. Tan(Θ) is 0.0262. Thus we would anticipate that the drum head would produce a time varying signal that is of order 0.0089, or about 0.89% fractional modulation below the non-varying ambient scattered light. The graphs indicate a peak of about 16% fractional modulation. The much higher observation is likely due to the fact that latex is a non-Lambertian scatterer, and we observed near the specular point, which while weak, is present in the BRDF of latex. This was done to collect the easily interpreted images shown above. In retrospect, this experiment benefited (this was not planned) from the comparatively steep slope of the BRDF at this point (3^o between source and detector, evenly split with respect to the membrane) for non-Lambertian surfaces.

The images in Figure 14 of the average image and of the computed fractional modulation from the inflated, and deflated states do illustrate the passive optical detection of the 0,1 mode as a limb brightened result as expected, with the surface curvature yielding a radially varying fractional modulation as expected. The small irregularity is because of the 3^o offset between source and detector. There is interesting small scale structure, which is a subject of further work, probably indicative of sensitivity to surface irregularity of the membrane, and the centroids are slightly offset because the camera and light source are slightly offset.

8. SUMMARY

We have explored the complexities of the reflected and scattered light using the "BRDF" as defined by Nicodemus with a focus on temporally varying phenomena. We have discussed what we might term baseline modulation of a vibrating surface with pure Lambertian scattering from changing irradiance of each infinitesimal unit surface area alone. We have demonstrated this by optically imaging detection of modulation resulting from the excitation of the 0,1 mode in a circular membrane. We have also discussed the effects of more realistic non-Lambertian scattering surfaces, and we have demonstrated optical imaging detection of transients using both effects. We have discussed some of the complexities in the scattering physics of vibrating surfaces, with an emphasis on physics-based phenomena that may affect the optical signal modulation of light scattered from a vibrating surface. As is usual, we have raised more questions than we have answered, which is what makes science interesting.

9. QUESTIONS FOR FUTURE RESEARCH

1. What fraction of the detected intensity modulation is from surface normal deflection (irradiance)?
2. What are the time dependent intensity modulation effects from a non-Lambertian BRDF?
3. What fraction of the detected intensity modulation is from geometrical shadowing?
4. What fraction of the detected intensity modulation is from lighting shadowing?
5. What are the time dependent intensity modulation effects from texture?
6. For each of these variables, can we quantify parameters and construct a physics based BRDF model that permits us to predict the detected fractional modulation from any given surface?

10. **Acknowledgments**:

This work was made possible with support from:
AFOSR under contracts FA9553-13-M-0055 and FA9453-14-C-0065
ONR under contract N00014-13-P-1209
AFRL under contract FA9453-12-C-0141
SSI under an in house research project
and we thank each of these sponsors! AFRL Public release # 377ABW-2014-0577. ONR Public release #43-448-14

References:

[1] Nicodemus, J.C., Richmond, J.J. Hsia, I.W. Ginsberg, and T. Limperis, F.E., "Geometrical Considerations and Nomenclature for Reflectance," U.S. Government Printing 0ffice Stock No. 003-003-01793, U.S. NBS Monograph 160, NBS (1977)

[2] Maurer, J., "Retrieval of surface albedo from space," U.Hi., http://www2.hawaii.edu/~jmaurer/albedo/, (2002)

[3] Clark, F.O., "Remote Passive Measurement of Information Including Engine Shaft Speed," Patent 8284405, (2012)

[4] Clark, F.O., "Remote Passive Detection of Surface Vibration," Patent 8488123, (2013)

[5] Clark, F.O., "Remote Optical Sensing of the Integrity of a Structure Using Reflections from the Structure," Patent pending, (2014)

[6] Pereira, W., Noyes, B., Noah, P., Pacleb, C., Clark, F., Dalrymple, S., Jeong, L., Westphal, A., "Hypertemporal Imaging Diffuse Modulation (HTI-DM) Experiment," AFRL-RV-HA-TR-2011-1010, 28 February (2011)

[7] Hay, J.R., Kielkopf, J.F., Clark, F.O., "Non-Contact Stand-off Optical Sensing of Cable Vibrations for Monitoring Structural Health of the William H. Harsah Bridge, CSX Eastern Parkway Overpass, The Sherman-Minton Ohio River Bridge at Louisville, KY," [Proc. 15th International Conference Experimental Mechanics] (ICEM15) (Porto, Portugal) July (2012)

[8] Kielkopf, J.F., and Hay, J. "System and method for precision measurement of position, motion, and resonances," Patent 8693735, (2014)

[9] Chandrasekhar, S., [Radiative Transfer], Oxford University Press (1950)

[10] Kielkopf, J.F., and Clark, F.O., "Fluctuations in Scattered Light" in preparation (2014)

[11] Schlick, C., "A Survey of Shading and Reflectance Models," [Computer Graphics Forum], v13, p121-132, June (1994)